



Cogging Torque Reduction in PMSM Motor by Using Proposed New Auxiliary Winding

K. Abbaszadeh^{1*} and S. Maroufian²

1- Associate Professor, Department of Electrical Engineering, K.N. Toosi University of Technology, Tehran, Iran

2- MSc. Student, Department of Electrical Engineering, K.N. Toosi University of Technology, Tehran, Iran

ABSTRACT

Performing fast and accurate methods for modeling the electrical machines has been the subject of several studies and many authors proposed different procedures to attain this aim. Beside the accuracy, the speed of the method is of great concern. On the other hand, the capability of the method to be changed according to the need is another important issue. Finite Element method provides relatively accurate results but it is time consuming and changing the parameters, once the model designed is difficult to be done. Magnetic Equivalent Circuit method is rather a new concept to model the electrical machines. The most important feature of the method is its flexible accuracy which can be determined due to the user's desire. Another important characteristic is the capability of the method in changing parameters. In this paper, a permanent magnet synchronous motor is modeled using Magnetic Equivalent Circuit; the values of the magnetic flux density and magnetic field intensity are calculated. Afterward, the generated output torque is calculated using Maxwell Stress Tensor. The comparison between the results of the MEC model and the Finite Element Analysis reveals the sufficient accuracy of the proposed method. Finally, a new method is proposed for cogging torque minimization which is based on the torque pulsation originated from an auxiliary winding. The result shows a significant reduction in the amplitude of the cogging torque.

KEYWORDS

PMSM Motor, Cogging Torque, Auxiliary Winding.

*
Corresponding Author, Email: Abbaszadeh@kntu.ac.ir

1-INTRODUCTION

Several methods are presented in papers for the analysis of electrical machines. A precise model should take into account different aspects of a machine structure to meet the desired accuracy. Some features like the cogging torque [1], [2], are strictly dependent on the machine physical features, like the number of poles and slots [3], pole arc to pole pitch ratio [3] and so on. Thus, such aspects and parameters should be included in the model for cogging torque analysis. On the other hand, the model should be fast enough and have the capability of parameter variation. Variation of the parameters will be useful in case of fault analysis and diagnosis [4] and also optimization.

Among the methods, FEA is the most accurate one but it is also time consuming [5]. Moreover, once the model is designed, changing the parameters will be difficult [6]. That is why researchers have always been searching for new methods which might be less accurate than FEA but rather faster. Winding Function Theory [7] and Magnetic Equivalent Circuit Method [5], [8], [9] are the examples of less accurate but faster methods. Several authors have done modifications on these methods to make them even faster and more accurate [5], [10], [11]. These modifications in some cases have added up some new capabilities to the previous methods [7].

Cogging torque, which arises from the variation of the magnetic field energy stored in the air gap, [3] is a drawback of Permanent Magnet motors. Many authors proposed different methods for analysis and reduction of cogging torque [2], [3], [12]. First of all, its characteristic and parameter dependency should be thoroughly analyzed; afterward, proper modification in the machine structure [1], [2], [3] will lead to the cogging torque minimization.

In this paper, a Magnetic Equivalent Circuit of a Permanent Magnet Synchronous Motor is first proposed. This model will provide data which are necessary for torque calculation and analysis. Based on the proposed method, Maxwell Stress Tensor has been used to calculate the output torque and thus cogging torque. The second part of the paper proposes a new approach to minimize the cogging torque. In this method, an auxiliary winding is added to the machine structure, thus a double excited motor is achieved. The torque pulsation will be used to mitigate the cogging torque pulsation as a result of this auxiliary winding. The auxiliary winding will decrease the cogging torque by 60 percent. Finally, the results of the MEC model are validated with FEA. This comparison affirms the model accuracy and validity.

2-PERMANENT MAGNET SYNCHRONOUS MOTOR

In this section, the permanent magnet synchronous motor, that has been the case of this study, is introduced. This motor consists of 8 PM poles that are located on the rotor surface. The stator part has 24 slots that encompass

its winding turns. The motor is designed based on the analytical approaches. With this in mind the number of winding turns, proper current density, volume of the magnets and, etc. are determined. Table.1 provides some specific features of the motor structure. Fig.1 shows a view of the designed motor.

TABLE.1. MOTOR PARAMETERS

Parameter	Value
Rated Output Power	3 kVA
Stack Length	180 m
Stator Inner Diameter	128 mm
Rotor Outer Diameter	112 mm
PM Thickness	4 mm
Number of Winding Turns (per phase)	200

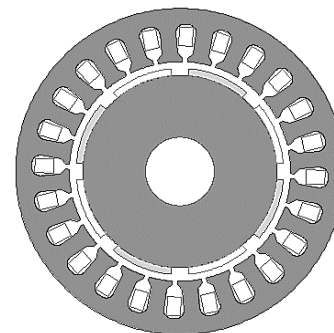


Fig.1. Permanent Magnet Synchronous Motor

3-MAGNETIC EQUIVALENT CIRCUIT MODELING

The basic principle of the Magnetic Equivalent Circuit Modeling is presented in this section. The main feature of the method is that its accuracy can be chosen by the one who applies the method. The machine structure is divided into elements called flux tubes [13]. Each flux tube carries uniform magnetic fluxes and thus has a magnetic reluctance which can be calculated according to the flux path, material and geometrical structure. After choosing the number of elements and their shapes, a reluctance network is generated. This reluctance network consists of several Magnetic Potential levels that solving the network will provide the value of the magnetic vector potential in each node of each level.

Modeling Process of the Motor Using Magnetic Equivalent Circuit

Based on the MEC principles, a reluctance network [9], [13] is generated for the PM motor. Fig.2 shows a schematic view of this reluctance network.

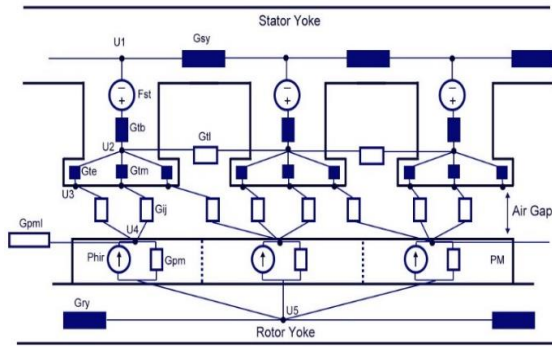


Fig.2. Reluctance network of the PM motor

Evaluating the cogging torque has been the final aim of this study; so special concern must be dedicated to the stator teeth as they play an important role in cogging torque. Each tooth tip has been divided into 3 elements for the better simulation of the reluctance variation while rotor rotation.

The reluctance network consists of five magnetic potential levels; $U_1 \sim U_5$. The value of the magnetic potential in each node is calculated using KCL's counterpart in the magnetic circuits. Beside the magnetic nodal equations, there are equations which relate winding currents to Magneto Motive Force (F_{st}) of teeth and Phase fluxes to teeth fluxes. Equations (1) and (2) show these relationships.

$$F_{st} = W'i \quad (1)$$

$$\varphi_{phase} = W''\varphi_{tooth} \quad (2)$$

Where W' and W'' are the magneto motive force transform matrix [13] and flux transform matrix, [13] respectively. These matrixes are determined due to the winding arrangement, number of turns, and etc.

These equations together with the nodal equations arrange a system of equations in which solving them results in the value of nodal magnetic potentials. Equation (3) shows an example of such nodal equation related to U_3 .

U_3 .

$$U_{3,1} \left(G_{te} + \sum_j G_{3,j}^1 \right) - U_{2,1} G_{te} - \sum_j U_{4,j} G_{4,j}^1 = 0 \quad (3)$$

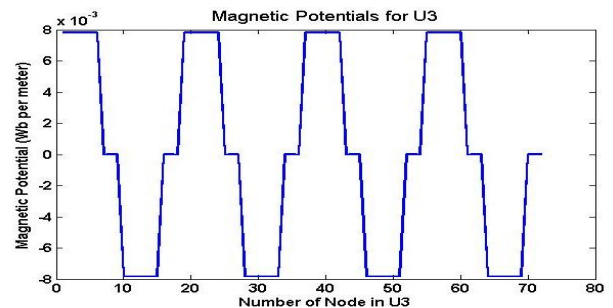
Where $U_{3,1}$ indicates the node number one of the third magnetic potential level; G_{te} is the permeance of the tooth edge which connects U_3 to U_2 . $\sum_j G_{3,j}^1$ is a summation of all permeances in the air gap which are connected to $U_{3,1}$ in a specific time step. This summation will vary as the rotor rotates. Such nodal equations can be

written in the same manner for all nodes in different magnetic potential levels.

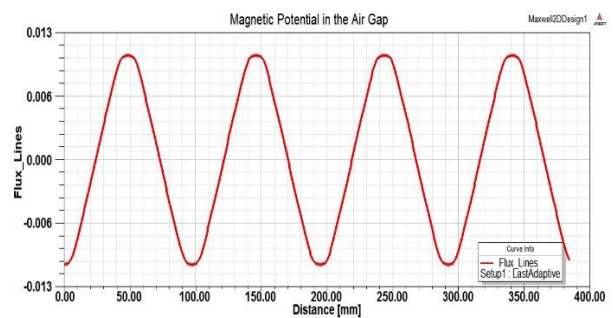
To solve the system of equations, an initial value must be assigned to some unknowns. In further steps, these initial values will be modified. The detail procedure of obtaining nodal equations is presented in [14].

The permeances located in the air gap are the most important ones as they are responsible for the energy conversion process. This part of the motor together with the stator teeth and PM poles should be precisely modeled to achieve an accurate and valid result. That's why this region is divided into smaller elements and thus the numbers of nodes are much more in comparison with the other parts. After solving the equations, the value of magnetic potential in each node of each level will be attained. Fig.3.a shows the magnetic potential level for U_3 in a time step. Fig.3. b shows the same result obtained from FEA.

The start point in Fig.3.a. is the first node located on a stator tooth. At this moment, this node is in front of the first node of the first PM. Moving from one node to another, the relative position of the stator teeth and rotor PMs will vary which are apparent in this figure.



(a)



(b)

Fig.3. Magnetic Potential in the Air Gap. a. calculated using MEC for 72 nodes below the stator teeth. b. calculated using FEA

The magnetic potential above each PM rises to a maximum value (positive or negative which indicates the magnetic potential vector direction). Between to PM poles, this value decreases to zero and then rises up again to the maximum for the next PM pole.

The MEC for the magnetic potential level of U_3 , which has been shown in Fig.3.a, possesses 72 nodes.

This limited number of nodes is the cause of the discrete result, thus the difference between MEC and FEA.

When the magnetic potentials of all nodes are determined, other magnetic parameters will be easy to calculate. Equation (4) is used to turn the magnetic potential into the magnetic flux density.

$$B = \nabla \times A \quad (4)$$

According to the machine structure, it's better to use cylindrical coordinate system to perform the above equation. So, the magnetic flux density will be calculated as follows:

$$B = \frac{1}{r} \begin{bmatrix} a_r & a_\varphi r & a_z \\ \frac{\partial}{\partial r} & \frac{\partial}{\partial \varphi} & \frac{\partial}{\partial z} \\ A_r & rA_\varphi & A_z \end{bmatrix} \quad (5)$$

On the other hand, the magnetic potentials only possess components along the z axis; that is the axis of the motor. With this in mind, the magnetic flux density will be calculated using equation (6)

$$B = \frac{1}{r} \left[a_r \frac{\partial A_z}{\partial \varphi} - a_\varphi r \frac{\partial A_z}{\partial r} \right] \quad (6)$$

It is apparent that the magnetic flux density only has components along r and φ axes, which is valid according to the Finite Element Analysis. Fig.4.a shows the magnetic flux density for the third magnetic potential level. Fig.4.b shows the same result which is calculated using the finite element analysis.

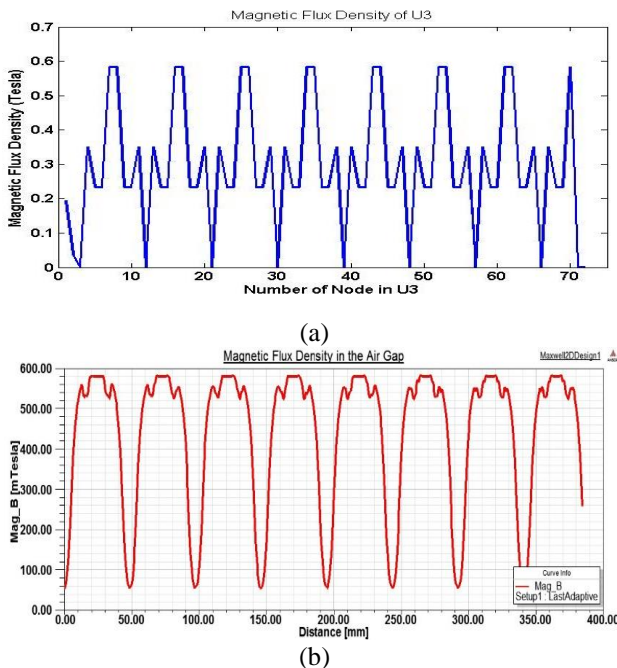


Fig.4. Magnetic Flux Density in the Air Gap. a. Calculated using MEC. b. Calculated using FEA

The slight difference between the two results arises from the fact that in the MEC model, the number of elements is limited to 72, so moving from one node to the adjacent node, in some cases causes higher jumps in the value; that some slight errors in the derivation process occur when compared to the FEA. Increasing the number of elements will solve this problem but the model complexity will also increase. So it is important to divide the machine structure into sufficient number of elements. This sufficiency will be evaluated while the output torque is calculated and compared to FEA result.

Up to this point, magnetic and electric characteristic of the designed motor are modeled using Magnetic Equivalent Circuit. The further step is to determine the output torque which is presented in the next section.

4-TORQUE CALCULATION AND ANALYSIS

A. OUTPUT TORQUE OF THE MOTOR

Several methods can be used to calculate the output torque of an electrical motor. Co-energy method [15], [16], Maxwell Stress Tensor [11], [15], [16], and Lorentz Force Theorem [15] are the methods that are mostly applied to maintain the output torque. Co-energy method is the easiest one and it is the most common method used in several papers [1], [3], [15]. Maxwell Stress Tensor is the most accurate and detailed one but it needs local knowledge about the magnetic field parameters. This feature makes this method proper to be applied for the results of the Magnetic Equivalent Circuit in order to calculate the output torque [11]. In this paper, Maxwell Stress Tensor has been applied to the obtained result of the MEC model, introduced in the previous section.

Output torque of a motor can be calculated using Maxwell Stress Tensor as follows: [15]

$$T = \frac{L_i}{\mu_0} \oint_l r B_n B_t dl \quad (7)$$

Where L_i is the stack length of the machine; r is the radius of the air gap; B_n and B_t are the radial and tangential components of the magnetic field density in the air gap, respectively; and l is the contour of integration, which is in this case, a path in the air gap of the motor, that encompasses the rotor and its magnets.

As / Since the results are discrete, equation (8) should be written in a discrete form [15]:

$$T = \frac{L_i}{\mu_0} \sum_i r^2 \int_{\theta_i}^{\theta_i+1} B_n B_t d\theta \quad (8)$$

In the above equation, θ_i indicates the angular position of the node which its components of magnetic field density are known. This integration will be done step by step for each node until one turn along the contour is passed. Fig.5.a shows the output torque of the motor

calculated using Maxwell Stress Tensor and MEC model. Fig.5.b is the same result calculated through using FEA.

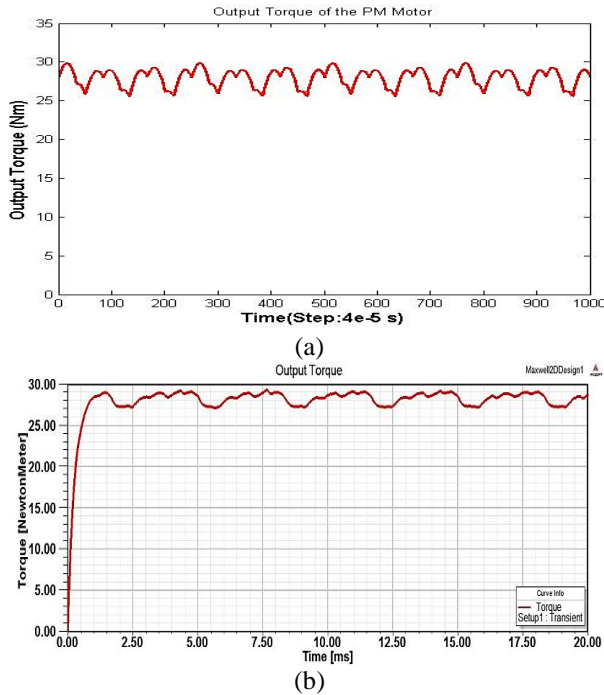


Fig.5. Output Torque of the Motor. a. Calculated using MEC and Maxwell Stress Tensor. b. Calculated using FEA

The amplitude of the output torque pulsation is about 1.6 Nm.

The MEC simulation is performed for 0.04 second, in this period of time, the motor rotates half a turn and the number of torque pulsations caused by the cogging effect is 12. The FEA simulation is performed for 0.02 second and thus, the number of cogging torque pulsations is 6.

The difference between the two results arises from the fact that the MEC model is not as accurate as the FEA, this is because of the limited number of nodes and some special features that might not be taken into account while using MEC. On the other hand, the procedure of motor starting is not modeled in MEC.

A. COGGING TORQUE REDUCTION

Cogging Torque is an issue mostly related to permanent magnet motors [1], [2], [3] which originate from the interaction of PMs and stator teeth [3]. As the rotor rotates, the amount of stored magnetic energy in the air gap changes and this results in a pulsation in the motor output torque. the cogging torque can be modeled in terms of stored magnetic co-energy variation: [3]

$$T_{cogging} = - \frac{\partial W}{\partial \theta} \quad (9)$$

In the above equation, W and θ are the magnetic co-energy and rotor angular position, respectively.

Using the mathematical relationships for the stored magnetic co-energy, one can define cogging torque, as follows:

$$T_{cogging} = \frac{1}{2} \varphi^2 \frac{d\mathcal{R}}{d\theta} \quad (10)$$

Where, φ and \mathcal{R} are the magnetic flux in the air gap and reluctance of the air gap, respectively.

According to this equation, cogging torque minimization can be done, alternating any of the parameters included in equation (10). Several authors proposed different methods to minimize the cogging torque [1], [2]. These methods are generally bifurcate; those which concentrate on the motor structure, like slot opening reduction [3], dummy slots [3], nonuniformly distributed teeth [17], magnet segmentation [18], and etc. and those which deal with the supply [19].

The proposed method in this paper is adding an auxiliary winding to the motor structure. This single phase winding is placed into the stator slots of the same motor and consists of 24 poles. The basic principle relies on the capability of a single phase winding to generate the pulsating torque. This pulsation is explained by the two magneto motive forces rotating in the similar speed but in different directions. The following relationship defines this phenomenon.

$$\mathcal{F} = \frac{1}{2} * \frac{4}{\pi} K_w \frac{N_t}{P} I_a [\cos(\omega t - \theta) + \cos(\omega t + \theta)] \quad (11)$$

Where K_w , N_t , P , I_a , ω , are the winding factor, number of winding turns, number of poles, amplitude of the current supplied, and the supply frequency, respectively.

The clockwise and counterclockwise components of the single phase winding magneto motive force can be shown using equations (12)

$$\begin{aligned} \mathcal{F}^+ &= \frac{1}{2} * \frac{4}{\pi} K_w \frac{N_t}{P} I_a \cos(\theta - \omega t) \\ \mathcal{F}^- &= \frac{1}{2} * \frac{4}{\pi} K_w \frac{N_t}{P} I_a \cos(\theta + \omega t) \end{aligned} \quad (12)$$

As these MMF waves pass by each other, a pulsation torque produces which its frequency is twice the frequency of the winding's supply. In order to maintain a pulsating torque with a proper frequency to deal with the cogging torque pulsation, the cogging torque pulsation frequency should be determined. As the rotor rotates along one slot pitch, the number of cogging torque ripples

N_s can be calculated using equation (13) [3]

$$N_s = \frac{2P}{HCF\{Q, 2P\}} \quad (13)$$

In this equation, P is the number of pole pairs and Q is the number of stator slots. HCF stands for the Highest Common Factor.

In this study, N_s is equal to 1, so when the rotor rotates a complete turn, 24 cogging torque ripples will appear; due to the motor's nominal speed, the cogging torque frequency is equal to 300 Hz; that is for cogging torque reduction with the help of the auxiliary winding, the frequency of the power supply to this winding must be 150 Hz, so that it would generate a torque pulsation with the frequency of 300 Hz.

Fig.6 shows the output torque of the motor after using the auxiliary winding.

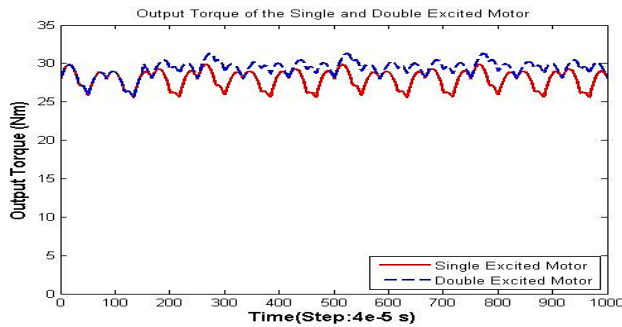


Fig.6. Output torque comparison of the single excited and double excited motor

In this figure, the dashed line shows the output torque of the double excited motor. The auxiliary winding is being supplied after 150 samples which equals to 6 milliseconds. In order to cancel the torque pulsation, the proper time for the current injection to the auxiliary winding and its power should be determined. These parameters are calculated using the Magnetic Equivalent Circuit designed previously. Fig.7 shows the MMF of the Auxiliary Winding.

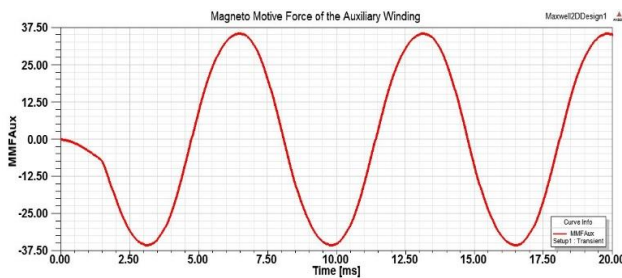


Fig.7. MMF of the auxiliary winding (Ampere turn)

The total number of turns of the auxiliary winding is 360.

To check out the validity of the MEC model, the auxiliary winding was placed on the FEA model, too. Fig.8 shows the same motor with the auxiliary winding. The effect of adding this auxiliary winding to the machine structure, on the output torque, is shown in Fig.9. In case of applying the auxiliary winding and supplying it with proper current, the torque ripple of the motor is 0.670 Nm which shows a 60 percent decrease in contrast with the main single excited motor

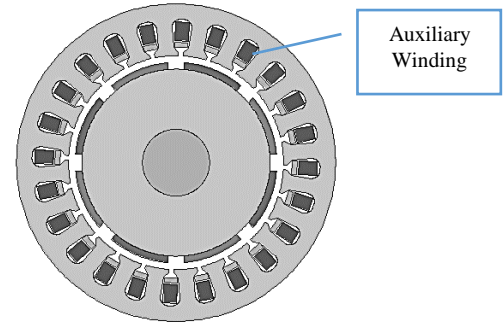


Fig.8. PM synchronous motor with the auxiliary winding

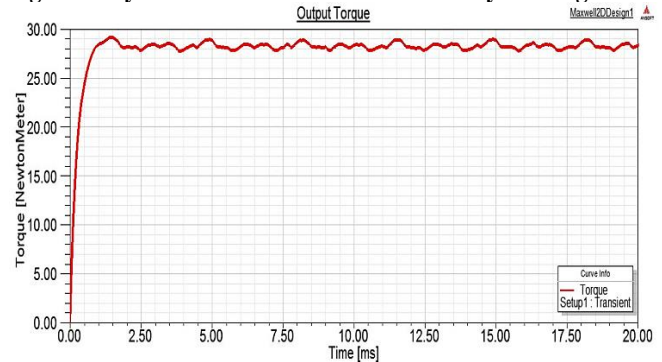


Fig.9. Output torque of the PM motor with the auxiliary winding

5-CONCLUSION

This paper can be divided into two separate parts; in the first part a permanent magnet synchronous motor is modeled using magnetic equivalent circuit. Obtained results of the MEC model, like magnetic potentials, magnetic flux densities, and output torque are compared to the results of the finite element analysis. This comparison reveals the validity and relative sufficient accuracy of the proposed model. In the second part, based on this magnetic circuit model a new method is proposed to minimize the cogging torque of the PM motor. Adding an auxiliary single phase winding to the machine structure generates a pulsating torque which interacts with the pulsation originated from the cogging effect. Proper design of the single phase winding can decrease the amplitude of the cogging torque by 60 percent.

REFERENCES

- [1]. Luke Dosiek, and Pragasen Pillay, "Cogging Torque Reduction in Permanent Magnet Machines", IEEE trans. Ind. Appl., Vol. 43, No. 6, pp. 1565-1571, Nov. / Dec. 2007.
- [2]. K. Abbaszadeh, F. Rezaee Alam, M. Teshnehlab, "Slot opening optimization of surface mounted permanent magnet motor for cogging torque reduction", Energy Conversion and Management 55 (2012) 108-115.
- [3]. Claudio Bianchini, Fabio Immovilli, Emilio Lorenzani, Alberto Bellini, Matteo Davoli, "Review of Design Solutions for Internal Permanent Magnet Machines Cogging Torque Reduction". Magnetics,

- IEEE Transactions on Vol.48 , Issue 10, pp 2685 – 2693, 2012.
- [4]. Karim Abbaszadeh, Seyede Sara maroufian, “PM Demagnetization Detection in Axial Flux Permanent Magnet Motor using ARX Model”, Electrical Engineering (ICEE), 2013 21st Iranian Conference
- [5]. Seyed Amin Saied, Karim Abbaszadeh, and Mehdi Fadaie, “Reduced Order Model of Developed Magnetic Equivalent Circuit in Electrical Machine Modeling”, IEEE Trans. Magn., Vol. 46, No. 7, pp. 2649-2655, July 2010.
- [6]. Ali Davoudi, Patrick L. Chapman, Juri Jatskevich, and Alireza Khaligh, “Reduced-Order Modeling of High-Fidelity Magnetic Equivalent Circuits”, IEEE Trans. power electronics, Vol. 24, No. 12, pp. 2847-2855, Dec. 2009.
- [7]. S. Saied, K. Abbaszadeh A. Tenconi, “Improvement to Winding Function Theory for PM Machine Analysis”, Proceedings of the 2011 International Conference on Power Engineering, Energy and Electrical Drives, pp. 1-6 11-13 May 2011
- [8]. Hamza W. Derbas, Joshua M. Williams, Andreas C. Koenig, and Steven D. Pekarek, “A Comparison of Nodal- and Mesh-Based Magnetic Equivalent Circuit Models”, IEEE Trans. Energy Convers., Vol. 24, No. 2, pp. 388-396, June 2009.
- [9]. T. Raminosoa, J.A. Farooq, A. Djerdir, A. Miraoui, “Reluctance network modelling of surface permanent magnet motor considering iron nonlinearities”, Energy Convers. and Manage. 50 pp 1356–1361, 2009.
- [10]. B. Sheikh-Ghalavand, S. Vaez-Zadeh, and A. Hassanpour Isfahani, “An Improved Magnetic Equivalent Circuit Model for Iron-Core Linear Permanent-Magnet Synchronous Motors”, IEEE Trans. Magn., Vol. 46, No. 1, pp. 112-120, Jan. 2010.
- [11]. Marco Amrhein, and Philip T. Krein, “Force Calculation in 3-D Magnetic Equivalent Circuit Networks With a Maxwell Stress Tensor”, IEEE Trans. Energy Convers. Vol. 24, No. 3, pp. 587-593, Sep. 2009.
- [12]. S. Saied, K. Abbaszadeh, A. Tenconi and S. Vaschetto, “New Approach to Cogging Torque Simulation Using Numerical Functions”, Industry Applications, IEEE Transactions on, Vol. 50, Issue: 4, pp 2420 – 2426, 15 July 2014.
- [13]. V. Ostovic, “Dynamics of Saturated Electric Machines”. New York: Springer-Verlag, 1989.
- [14]. Karim Abbaszadeh, Seyede Sara Maroufian, “Axial flux permanent magnet motor modeling using magnetic equivalent circuit”, Electrical Engineering (ICEE), 2013 21st Iranian Conf.
- [15]. Jacek F. Gieras, Mitchell Wing, “Permanent Magnet Motor Technology, Design and Applications, Second Edition, Revised and Expanded”, CRC Press, 2005.
- [16]. Y. G. Guo, J. G. Zhu, and V. S. Ramsden, “calculation of cogging torque in claw pole permanent magnet motors” Fourth International Conference on Industrial and Information Systems, ICIS 2009, 28 - 31 Dec. 2009.
- [17]. Daohan Wang, Xiuhe Wang, Dongwei Qiao, Ying Pei, and Sang-Yong Jung, “Reducing Cogging Torque in Surface-Mounted Permanent-Magnet Motors by Nonuniformly Distributed Teeth Method”, IEEE Trans. Magn. Vol. 47, No. 9, pp. 2231-2239, Sep. 2011
- [18]. Ramdane Lateb, Nouredine Takorabet, and Farid Meibody-Tabar, “Effect of Magnet Segmentation on the Cogging Torque in Surface-Mounted Permanent-Magnet Motors”, IEEE Trans. Magn., Vol. 42, No. 3, pp. 442-445, March 2006.
- [19]. M. rahimi, N. talebi, k. abbaszadeh, S.M.T. bathae, “Simple Harmonic Compensation Method for Torque Ripple Minimization in PMSM Drives”, Fourth International Conference on Industrial and Information Systems, ICIS 2009, 28 - 31 Dec. 2.